

# The Edinburgh/Durham Southern Galaxy Catalogue – IX. The Galaxy Catalogue

Robert C. Nichol<sup>1,3,4</sup>

Department of Physics, Carnegie Mellon University, 5000 Forbes Ave., Pittsburgh,  
PA-15213, USA

Christopher A. Collins<sup>1,2</sup>

Astrophysics Research Institute, Liverpool John Moores University, Twelve Quays House,  
Egerton Wharf, Birkenhead L41 1DL, UK

Stuart L. Lumsden<sup>1,5</sup>

Department of Physics and Astronomy, University of Leeds, Leeds LS2 9JT, UK

Received \_\_\_\_\_; accepted \_\_\_\_\_

Submitted to the Astrophysical Journal Supplement Series

---

<sup>1</sup>Royal Observatory Edinburgh, Blackford Hill, Edinburgh, EH9 3HJ, UK

<sup>2</sup>Department of Physics, Science Laboratories, South Road, Durham DH1 3LE, UK

<sup>3</sup>Department of Physics & Astronomy, Northwestern University, Dearborn Observatory,  
2131 N. Sheridan Road, Evanston, IL-60208, USA

<sup>4</sup>Department of Astronomy & Astrophysics, University of Chicago, 5640 S. Ellis Avenue,  
Chicago, IL-60637, USA

<sup>5</sup>Anglo-Australian Observatory, P.O. Box 296, Epping, NSW 1710, Australia

## ABSTRACT

We announce here the public availability of the Edinburgh/Durham Southern Galaxy Catalogue (EDSGC, <http://www.edsgc.org>). This objective galaxy catalogue was constructed using the COSMOS micro-densitometer at the Royal Observatory Edinburgh and constitutes one of the largest digitized galaxy surveys currently in existence. The EDSGC contains a total of 1,495,877 galaxies (each with 27 image parameters) covering an contiguous area of  $1182\text{deg}^2$  centered on the South Galactic Pole. The data consists of photographic  $b_j$  magnitudes calibrated via CCD sequences which provide a plate-to-plate accuracy of  $\Delta b_j \simeq 0.1$ . Extensive external checks have demonstrated that the global EDSGC photometry is free of large-scale systematic gradients and is therefore, ideal for studying the distribution of galaxies on large angular scales. Independent spectroscopy of EDSGC galaxies has shown that the accuracy of the star-galaxy separation is consistent with earlier visual checks and that only 12% of EDSGC galaxies are potentially mis-classified. This paper is intended to provide a summary of the essential details of the catalogue's design and construction as well as provide a brief summary of the main scientific achievements using the EDSGC over the last ten years.

*Subject headings:* surveys – galaxies: general – galaxies: photometry – cosmology: observations

## 1. Introduction

Surveys of galaxies are invaluable tools for cosmologists. To date, the most comprehensive catalogues of galaxies have resulted from the optical photographic surveys carried out with the Schmidt telescopes at the Palomar and Anglo–Australian Observatories. The earliest of these surveys were visually compiled counts of galaxies, the largest being the Lick catalogue of galaxies which presents counts in cells of  $10 \times 10$  arcminutes for some 800,000 galaxies covering two thirds of the entire sky. The complementary Abell cluster catalogue (Abell, Corwin & Olowin 1989) is an amalgamation of Abell’s original northern cluster catalogue (Abell 1958), carried out with the Palomar Sky Survey 103a–E plates, with the southern extension using the IIIa-J Southern Sky Survey plates taken by the UK Schmidt at Siding Springs. The final all–sky Abell catalogue consists of 4073 rich clusters of galaxies each having at least 30 members with a nominal redshift of  $z \leq 0.2$  and is the first serious attempt to systematically categorize the properties of galaxy clusters. The Abell catalogue remains the most widely used cluster catalogue in the astronomical literature.

The early 1990s saw the completion of the first large-scale digitized galaxy surveys. These combined the best available photographic material, in the form of UK Schmidt IIIa-J photographic survey plates, with digitization technology in the form of fast micro-densitometers *e.g.* the COSMOS machine in Edinburgh and the APM machine in Cambridge. The digitization process overcomes the inherent subjectivity of ‘eyeball’ surveys and the impact of the resulting galaxy catalogues has been extensive (see Section 3).

As we enter a new millennium, the number and size of galaxy surveys will expand rapidly due to new photographic galaxy surveys (*e.g.* DPOSS, Djorgovski et al. 1998; SuperCOSMOS, Phillipps et al. 1998) and CCD surveys (*e.g.* SDSS, York et al. 2000). These new surveys will supersede the presently available galaxy catalogues because of their increased sensitivity, areal coverage, color information and more accurate photometry.

Therefore, in this paper, we announce the public release of the Edinburgh/Durham Southern Galaxy Catalogue (EDSGC) to assist cosmological research and is now particularly timely given the completion of several redshift galaxy surveys for which the EDSGC has been the input object catalogue (see Section 4).

The structure of this paper is as follows: In Section 2, we discuss the construction of the EDSGC and describe the available parameters and catalogue characteristics. In Section 3, we outline the availability of the EDSGC and in Section 4, we present a summary of the supplementary data available in the EDSGC area. In Section 5, we present the extensive external checks that have been performed on the catalogue, while in Section 6, we review the science which has been carried out using the EDSGC.

## 2. The Edinburgh/Durham Southern Galaxy Catalogue

The Edinburgh/Durham Southern Galaxy Catalogue (EDSGC) is one of the first fully automated objective galaxy catalogues to be constructed. It covers an area of  $\simeq 1200\text{deg}^2$  centered on the South Galactic Pole (SGP) and contains extensive information on over one million galaxies. The majority of the initial work involved in its construction has already been presented in several places *i.e.* Collins, Heydon-Dumbleton & MacGillivray 1989, Heydon-Dumbleton, Collins & MacGillivray 1989 and Heydon-Dumbleton 1989. In this section we summarize the data and the methods used in the catalogue’s construction and presents some of the tests implemented on the completed EDSGC.

### 2.1. The Raw Data

The UK Schmidt Telescope (UKST) at Siding Springs in Australia was commissioned in late 1973 to carry out a systematic photographic survey of the southern hemisphere.

The UKST has a 1.8m diameter mirror with a 1.2m aperture which provides a large field of view making it ideal for the construction of such a large-area survey. The photographic plates used by UKST subtends an area of  $6.4^\circ \times 6.4^\circ$  on the sky with a plate scale of 67.12 arcseconds per millimeter. For all the surveys carried out by UKST, the centers of the plates are separated by  $5^\circ$  which provides a substantial overlap between them and removes the need to use the plate edges which are heavily vignetted (vignetting is negligible within  $2.7^\circ$  of the plate center).

The EDSGC is based on plates taken from the ESO/SERC Atlas. This atlas consists of glass copies of the SERC J survey which was the first survey to be completed by UKST and covers the whole southern sky below a declination of  $-17^\circ$  (606 plates in total). The passband of the SERC J survey is defined by the response of the emulsion (Kodak IIIA-J) combined with a Schott GG395 filter. This provides an almost uniform sensitivity in the wavelength range  $3500\text{\AA}$  to  $5400\text{\AA}$  and is close to the standard Kron-Cousins B passband. Image magnitudes on the plates are usually referred to as  $b_j$  magnitudes.

Both the original J survey plates and the atlas copies were taken using a strict set of criteria to minimize systematic errors between different plate exposures and, more importantly, to ensure that the process was highly repeatable. For example, survey plates were only taken in dark time, good seeing (less than 3 arcseconds) and with the sun  $> 18^\circ$  below the horizon to avoid astronomical twilight. During the exposure, each plate was held in a curved holder and was flushed with nitrogen to reduce the effects of differential desensitisation over the plate<sup>6</sup>. The developing and copying of the plates were also carried out with a high degree of consistency to ensure that systematic differences between plates were not introduced. Finally, quality control checks were carried out on all plates and

---

<sup>6</sup>We note here that a few EDSGC plates may have been taken before nitrogen-flushing was instigated

each was graded either A, B or C. Therefore, this atlas represented the most homogeneous catalogue of photographic plates available at that time. The reader is referred to the UK Schmidt Telescope Unit Handbook (1983) for a description of the procedures used in taking the original plates, Cannon et al. (1978) for full details of the processing of the plates and Bruck & Waldron (1984) for a discussion of the copying process.

In total, 60 grade A plates were used in the EDSGC and these are listed in Collins, Nichol & Lumsden (1992; CNL92). These plates were extracted from the ESO/SERC Atlas held in the UK Schmidt Library at the Royal Observatory Edinburgh and scanned by COSMOS, also at the Royal Observatory Edinburgh. The COSMOS machine was a high-speed flying spot micro-densitometer, specifically designed and constructed for scanning astronomical photographic plates (details of COSMOS can be found in MacGillivray & Stobie (1984) while the characteristics of its descendent, SuperCOSMOS, are to be found in Miller et al. 1991) . The COSMOS machine originally sat on a plinth driven 35 feet into the ground which separates it from the rest of the building thus preventing vibrations of any sort from effecting the scans. In addition, COSMOS and the UKST plate library were kept in a dust-free environment, thus reducing the chances of contamination on the plates.

Plates were fed into COSMOS with their south side at the top of the plate carriage holder and raster scanned using a beam of light from a cathode ray tube of width 8 microns. As the plate moved in the y direction, the beam scans in the x direction with a pixel size of 16 microns. In total, an area of  $287\text{mm} \times 287\text{mm}$  was scanned each time which corresponds to an area of  $5.35^\circ \times 5.35^\circ$  on the sky. For each pixel, a transmission value was calculated by comparing the light measured passing through the plate with a reference signal. This in turn, was converted into a measured intensity using a Baker density calibration curve (MacGillivray & Stobie 1984).

COSMOS was operated in two modes; mapping and threshold. The first recorded all

the pixel information on a plate and therefore required a vast amount of computer storage. The second recorded only pixels that were a certain percentage above the sky background of the plate (the typical sky background for these plates is  $\simeq 22.3$  magnitude per square arcsecond in the photographic  $b_j$  system). This is determined beforehand by scanning the plate with a much lower resolution (32 microns) to measure the large scale variations over the plate which are usually due to a combination of large nearby stars, vignetting and differential desensitisation. After scanning, the pixel data was passed into the COSMOS image analyzer (see Beard, MacGillivray & Thanisch 1990) which connects all adjacent pixels producing a final set of objects for each plate. Each image was then assigned 27 individual image parameters such as the image magnitude, position and both the intensity weighted and unweighted moments of the pixel distribution (Stobie 1980 and Section 3 below). Plates used in the EDSGC were scanned in threshold mode, with a threshold of 8% to 10% above the sky background. This ensured that there were approximately the same number of objects in each scan and was found by MacGillivray & Dodds (1982) to be an acceptable level for maximizing the number of true images compared to ‘noise’ images.

The magnitudes returned by COSMOS were isophotal magnitudes and the threshold quoted above for the EDSGC corresponded to a final isophote of 25 magnitudes per square arcsecond in  $b_j$ . For images brighter than  $b_j = 20.5$ , the magnitudes were effectively total magnitudes (MacGillivray & Dodds 1982). In addition, the measured magnitudes depend upon the sky background magnitude of the scanned plate and adopting a fixed detection threshold for all the plates introduced large variations between the zero-point magnitudes of the plates. Therefore, it was imperative to obtain external photometry to calibrate the magnitude scale of each plate.

All the COSMOS scans used in the EDSGC were analyzed using the COSMOS de-blending software (Beard et al. 1990), which involved re-thresholding each image in

intensity space at 8 progressively higher thresholds in search of saddle-points in the image's intensity distribution. If such saddle-points were found, the separate peaks were fitted by Gaussians and split into their daughter images. At the SGP, the number of blended objects was found to be  $\simeq 10\%$  at all magnitudes and implementing the de-blending software substantially reduced this number *e.g.* at a surface density of 20 galaxies per square arcminute (*e.g.* the cores of rich clusters) the number of real objects detected increased by over 30% because of de-blending (Heydon-Dumbleton et al. 1989). De-blending of the images was vital to the EDSGC for two reasons. First, faint star-star mergers near the plate limit imitated galaxies because their combined shape appeared elliptical and they had a lower surface brightness compared to a single star. If these were not de-blended, then there would have been a significant contamination of false galaxies at faint magnitudes. Secondly, the EDSGC was used in the construction of an automated cluster catalogue (Section 6). If de-blending had not been implemented, the cores of many rich clusters would have appeared as single large objects and therefore, would not have been detected by the automated cluster detection algorithm.

### *2.1.1. Star-Galaxy Classification*

A detailed discussion of the COSMOS star-galaxy separation criteria can be found in Heydon–Dumbleton et al. (1989). However, for completeness, we give an overview of the techniques here.

A COSMOS scan of a typical Schmidt plate contains on average 200,000 objects. To the plate limit, over 90% of these objects are stars which clearly must be removed to produce a reliable and meaningful galaxy catalogue. For the EDSGC, this was achieved using 3 parameters defined during the scanning of the plates. Each parameter worked over a different magnitude range and their combined effect covered the full range of magnitudes



observed on a plate.

These 3 classifiers were: The G classifier which works for magnitudes brighter than  $b_j \simeq 16$  and effectively measures how well an object fills the ellipse fitted to it (for stars brighter than  $b_j \simeq 16$ , diffraction spikes dominate the fitted ellipse but they have a relatively small area, while galaxies at this magnitude tend to fill their fitted ellipse): The Log-area classifier which works at intermediate magnitudes ( $16 < b_j < 19.5$ ) and relies on the fact that galaxies have a lower surface brightness than stars: The S classifier which works for magnitudes fainter than  $b_j = 19.5$  by comparing the measured size of the image to that expected for a Gaussian point-spread function.

Near the limit of the plates, star-galaxy separation became extremely difficult. Therefore, COSMOS scans used in the EDSGC were cut at a COSMOS magnitude of -1.0, which roughly corresponded to  $b_j \sim 21$  for most plates. To test the reliability of the star-galaxy separation, visual checks were carried out on 5 plates spread across the EDSGC. For each plate, 300 classified galaxies and 300 classified stars, over a broad range in magnitude, were randomly selected and visually inspected. The result of this test was a  $> 95\%$  completeness for the galaxies at all magnitudes with  $< 10\%$  stellar contamination. Similar results were obtained for visual checks on images selected before and after de-blending. For a much fuller discussion of these classifiers, their effective magnitude ranges and the visual tests the reader is referred to either Heydon-Dumbleton et al. (1989) or Heydon-Dumbleton (1989).

### *2.1.2. Photometric Calibration*

As stated above, COSMOS only returned the magnitude of objects relative to the background magnitude limit of the plate. Therefore, it was essential to obtain external

photometry to calibrate all the galaxies in the EDSGC by determining the sky background magnitude or zero-point magnitude of the plates. For galaxies, the relationship between the COSMOS magnitude and the  $b_j$  magnitude is linear over a wide range of magnitudes and can be represented by  $b_j = m_{cosmos} + m_{sky}$  where  $m_{cosmos}$  is the instrumental magnitude (and negative) and  $m_{sky}$  is the constant sky background of the plate (see below and Table 1).

The EDSGC was calibrated using CCD direct images obtained at CTIO and SAAO. In total, 31 calibration sequences were taken across the whole EDSGC and were spaced in a “checker board” fashion i.e. plates either had a sequences on them or overlapped with two or more plates with a sequence on. Each CCD frame was centered on a loose cluster which resulted in  $\sim 15$  usable galaxies per frame for the calibration. For the plates with a sequence, the COSMOS magnitudes of the observed galaxies were plotted against their CCD magnitudes and from the fit (with the slope fixed at 1.0)  $m_{sky}$  was obtained. These zero-points were then used to calibrate the whole of the plate with a uncertainty of  $\sim 0.05$  magnitudes. In Table 1, we present our measured  $m_{sky}$  values for the 31 EDSGC plates with a CCD sequence. Plates marked with an asterix have an uncertain calibration and should be viewed as preliminary at present. For plates without a sequence,  $m_{sky}$  was calculated using the galaxies in the overlap regions with plates with a sequence (typically 1000-3000 galaxies in each overlap). On average, each uncalibrated plate overlapped with 2-3 calibrated plates which prevented erroneous calibrations from propagating through the survey (see our discussion of edge plates below).

The histogram of measured plate magnitude offsets between adjacent plate zero-points is presented in CNL92 and the best fit Gaussian to this distribution has a dispersion of 0.08 magnitudes. This implies a calibration uncertainty of 0.05 magnitudes on each plate which is within the limits set by Geller, Kurtz & de Lapparent (1984) for plate matching errors

for any new galaxy catalogue used in measuring the large scale distribution of galaxies. Once again, the reader is referred to Heydon-Dumbleton (1989) and Nichol & Collins (1993) for a more detailed description of the photometric calibration of the EDSGC and a fuller discussion of the errors.

## 2.2. Final Catalogue

### 2.2.1. Spurious Detections and Systematic Errors

Before the plates were joined to form one homogeneous catalogue, the individual COSMOS scans were cleaned of spurious objects. The main source of such objects was from the accidental de-blending of star halos around bright stars in the field ( $b_j < 12$ ) which tended to mimic rich clusters of galaxies. To combat this effect, the areas around stars brighter than  $m_{cosmos} = -9$  were removed or “drilled” with a radius of 6.7 arcminutes (UKST handbook 1983). The exact magnitude used to select the stars was obtained from the plots of the G parameter against magnitude. In total, 553 such “drill holes” were made and a full list of these holes can be found on the EDSGC webpage.

Other spurious objects were produced by ghosts from very bright stars ( $b_j \sim 6$ ) in the field, satellite trails, large nearby galaxies and dense star clusters. Therefore, we plotted the galaxy distribution on each plate and visually inspected these plots for any suspicious features (*e.g.* very dense clusters of galaxies etc.). Such features were then inspected on the original glass plates to determine if they were real astronomical objects or errors as discussed above. If they were spurious, the data around these objects was interactively removed from the catalogue. In particular, Fields 404, 356 & 469 had large star ghosts which were drilled with a radius of 40 arcminutes and Field 466 had a large de-focussed region in the northwest corner of the plate. This area was removed as no alternative plate

existed with a comparable overall quality. In total, 10 interactive drill holes were used in the EDSGC and their positions, with comments, are given in Table 2.

Another source of contamination in the catalogue came from satellite trails. From the visual checks of the galaxy distribution of the plates, 11 plates were found to have this form of contamination. Combined with this, there were also spurious galaxies associated with the de-blending of diffraction spikes of stars. Both these types of spurious image were removed using the fact that they had preferentially aligned position angles i.e. diffraction spikes of stars were aligned with the edges of the plate and therefore, their position angles were always  $0^\circ$ ,  $90^\circ$  or  $180^\circ$ . In addition, these images have high ellipticities and filled their fitted ellipse extremely well. Therefore, on the plates in question, all detected objects were plotted in the eccentricity (minor over major axis) versus position angle plane which cleanly separated the satellite trails from the majority of other objects. A cut was made in eccentricity (typically between 0.3 and 0.4) and all objects with a lower value than this cut were plotted in the log–area versus magnitude plane (*i.e.* as used for star–galaxy separation). As discussed above, the real galaxy population stood away from the spurious population and the two were separated simply using a straight line. This method was very effective at removing the satellite trails and diffraction spikes, with typically 500 images removed on each plate. As a check, the objects both rejected and re-accepted into the catalogue by this methodology were visually inspected on 5 of the 11 affected plates. Of rejected images,  $\sim 8\%$  were galaxies, while for the re-accepted images, over 95% were galaxies. Due to the success of this method in removing residual diffraction spikes, it was performed on all the plates in the EDSGC and on average  $\sim 100$  objects were removed per plate. Visual checks of these rejected objects were in agreement with the numbers quoted above.

Once all the plates had been photometrically calibrated and cleaned of spurious objects,

the individual COSMOS scans were mosaiced together to produce a final homogeneous catalogue of galaxies. This was achieved interactively because the extent of the overlap between different pairs of plates varied extensively. The western edges of the UK Schmidt plates suffered the worst vignetting and desensitisation (UKST handbook 1983), while the northern edges displayed a systematic excess of faint galaxies which seemed to be a problem with the COSMOS calculation of the plate background intensity near that edge. This systematic excess was not due to the image classification or the photometric calibration because the effect was still present in the raw COSMOS scans (however, we note it only effected the first few lanes of the COSMOS scan and was therefore, only effected a small area of the plate). The EDSGC plates were attached together with a preference towards the eastern edges of the plates into long strips of fixed declination, which were then added together with a preference given towards the southern edges of these strips.

### 2.2.2. Areal Coverage

The EDSGC contains 1,495,877 galaxies taken from 60 Schmidt survey fields as listed in Table 2 of CNL92. The largest contiguous region within the EDSGC (avoiding the complicated plate boundaries of the EDSGC) is given by:  $3^{hrs}$  to  $22^{hrs}$  (through  $0^{hrs}$ ) and  $-23^\circ$  to  $-42^\circ$  (B1950). This gives a total area of  $1182\text{deg}^2$  and should be used as the EDSGC window function *i.e.* we recommend users confine themselves to this region for all statistical analyses. This was the region used by CNL92 for the galaxy angular correlation function.

### 3. Availability of the EDSGC

The EDSGC is available for download over the internet from <http://www.edsgc.org>. On this webpage, there are two catalogue available: The first is a smaller version of the EDSGC with only 7 attributes (see Table 3) and the full EDSGC with 27 attributes (see Table 4). In Tables 3 and 4, column 1 gives the name of the attribute, Column 2 gives the units of the attribute and Column 3 is a short description of the attribute. It is worth re-iterating here that the plate scale of the UK Schmidt Telescope is 67.12 arcseconds per millimeter giving 1.07 arcseconds per COSMOS pixel. These numbers will allow users of the EDSGC to convert some of the catalogue attributes into astronomically meaningful values.

### 4. Supplementary Information on the EDSGC

Over the past decade, there has been significant auxiliary information gathered in the EDSGC area. Such data includes the Las Campanas Redshift Survey (LCRS; Shectman et al. 1996), the ESO Nearby Abell Cluster Survey (ENACS; Katgert et al. 1996), the ESO Slice Project (ESP; Vettolani et al. 1997) and the Durham/UKST Redshift Survey (DURS; Ratcliffe et al. 1998). The former two surveys provide serendipitous information while the latter two redshift surveys use the EDSGC, or a subset of the survey, as their input catalogues. In total, there are 12,888 EDSGC unique galaxy redshifts from these four surveys (5996 from LCRS, 3836 from ESP, 2501 from DURS and 907 from ENACS) and we make these data available on the main EDSGC webpage (see <http://www.edsgc.org>). Only 176 EDSGC galaxies have more than one redshift measurement from these four different redshift surveys and, for these galaxies, the mean absolute difference in redshift is  $71\text{km s}^{-1}$  (the largest observed difference is  $306\text{km s}^{-1}$ ).

## 5. External Checks

### 5.1. Photometry

Extensive checks of the internal photometric calibration of the EDSGC were carried out in Heydon-Dumbleton (1989). These checks centered around the examination of galaxies in the overlap regions of plates and on the galaxy number counts as a function of right ascension and galactic latitude. These internal tests showed no evidence for systematic calibration errors in the EDSGC.

In this section, we investigate external checks of the EDSGC photometry since as demonstrated in Nichol & Collins (1993) systematic plate-to-plate photometric errors can significantly affect the form of the galaxy angular correlation function (see CNL92). Therefore, it is important to have a homogeneous magnitude system across the whole EDSGC.

#### 5.1.1. *External $b_j$ CCD data*

In Nichol (1993), we presented two external checks of the EDSGC photometry. The first of these used the published CCD photometric calibration sequences of the APM galaxy survey (Maddox, Efstathiou & Sutherland 1990a). At the bright end ( $b_j < 17$ ), the scatter in magnitude is large with a typical difference between the two surveys of  $\pm 0.2$  magnitudes. However, the majority of the comparison data are for galaxies fainter than a mean magnitude of  $b_j = 18$ . Over a range of 3 magnitudes, the data are consistent with the expected scatter due to the APM & COSMOS machine measuring errors ( $\sim 0.1$  magnitudes). The main result of this comparison is an overall 0.2 magnitude shift at all magnitudes between these two independent surveys, with the APM being the fainter of the two. A large part of this discrepancy could be the difference between total (APM) and

isophotal (EDSGC) magnitude measurements

In terms of the correlation analysis presented in CNL92, a simple shift in the global magnitude calibration between the APM and COSMOS catalogues is not a significant problem, since the angular correlation function is scaled by the observed number density of galaxies in the catalogue. A potentially more serious problem would be the existence of a variable magnitude shift as a function of plate position or right ascension, as this would introduce large scale gradients. To test for this, the mean magnitude shift of EDSGC plates with an APM sequence were investigated as a function of Right Ascension. As discussed in Nichol (1993), this analysis showed no signs of a systematic variation in the 0.2 magnitude shift between the two surveys across the whole EDSGC survey. This is supported by a linear fit to the data, which gives  $\Delta m_{APM-COSMOS} = (0.18 \pm 0.04) - (1.6 \pm 2.8) \times 10^{-2} \alpha$ , where  $\alpha$  is the right ascension of the EDSGC plate center (24 hours was subtracted for RA coordinates greater than 12 hours). This relationship predicts an offset of only 0.07 magnitudes between the two ends of the EDSGC, with a one sigma upper offset limit of 0.21 magnitudes.

In addition to the APM CCD sequences, Nichol (1993) used two CCD calibration sequences used by Matthew Colless in his study of the cluster luminosity function (Colless 1986). This comparison however does not show any systematic displacement between the EDSGC and Colless zero-points and is fully consistent with the expected scatter about zero given the COSMOS machine measuring error. In addition, the two Colless sequences (on Fields 349 and 405) are separated by nearly 2 hours in right ascension and show no evidence for a systematic shift in the EDSGC magnitude zero-points.



### 5.1.2. Other External Photometry Data

As outlined in Section 4, there are 5996 galaxies in common between the Las Campanas Redshift Survey (LCRS; Shectman et al. 1996) and the EDSGC. These galaxies were matched using a search radius of 4 arcseconds – centered on the EDSGC galaxy coordinates - which seemed appropriate based on our separation analysis. If an EDSGC galaxy had two, or more, possible match-ups, we forced there to be a unique match-up by simply taking the closest LCRS galaxy.

In addition to providing redshift measurements, the LCRS also published (Thuan-Gunn) r-band photometry on all their galaxies which allows us to study the large-scale distribution of galaxy colors ( $b_j - r$ ) across the entire EDSGC right ascension coverage *i.e.* the EDSGC overlaps with the  $-39^\circ$  and  $-42^\circ$  declination strips of the LCRS which span from  $\simeq 21^{hrs}$  to  $\simeq 4^{hrs}$  in right ascension. Therefore, this provides a significant external check of our photometry since, on average, galaxies should have the same  $b_j - r$  color across the survey, ignoring reddening effects, or real large-scale structure in the universe. We note here that we are not making any claims about the absolute  $b_j - r$  color of galaxies as this would require a detailed analysis of both the EDSGC and LCRS aperture photometry; we are simply examining the large-scale trends in the  $b_j - r$  color as a function of right ascension and original plate number

In Figure 1, we plot the  $b_j - r$  color of all galaxies as a function of right ascension. This plot immediately demonstrates that there is no large-scale systematic error between these two independent photometric systems *i.e.* the mean galaxy  $b_j - r$  color is a constant over 70 degrees in right ascension for this joint survey. This is more clearly shown in Figure 2a which plots the mean and standard deviation of the  $b_j - r$  color versus right ascension for the EDSGC-LCRS sample. The scatter between these mean points is significantly smaller than the intrinsic scatter seen in the individual galaxy colors (Figure 1) and is

fully consistent with the sum of errors on the individual photometric measurements *i.e.* as discussed above and in CNL92, the rms plate-to-plate scatter for the EDSGC is  $\Delta m \simeq 0.08$  (which does not include the photographic measurement error) while the standard deviation of pairwise galaxy magnitude differences for LCRS galaxies which were measured twice on overlapping “bricks”<sup>7</sup> is  $\sigma_m = 0.10$ , for  $16.0 < r \leq 17.0$ , and  $\sigma_m = 0.17$ , for  $17.0 < r \leq 18.0$  (see also Figure 3 of Shectman et al. 1996).

To investigate this further, we have plotted in Figure 2b the mean  $b_j - r$  color for the EDSGC–LCRS galaxies as a function of their original EDSGC plate identification and right ascension (there are only LCRS data on 14 of the original 60 EDSGC plates). In this plot, we present the mean EDSGC–LCRS galaxy color for each plate as a function of the mean right ascension of that plate. We have broken the data into the two different LCRS declination slices, *i.e.*  $-39^\circ$  and  $-42^\circ$ , since the former of these two runs through the center of the EDSGC plates (where the calibration is expected to be best), where the latter runs across the southern edge of the EDSGC (as discussed in Section 2.2.2, we cut the EDSGC at  $-42^\circ$  for statistical analyses).

Figure 2b once again demonstrates that there is no large-scale gradient between the two photometric systems. The amplitude of the scatter seen between the mean EDSGC–LCRS galaxy color for  $-39^\circ$  declination strip is fully consistent with the rms scatter quoted above and in CNL92.

We note here that the larger scatter seen in Figure 2b for the  $-42^\circ$  LCRS declination strip is probably due to photographic plate edge effects. Such edge effects have little consequence on the science of the EDSGC, as outlined in Section 6, since in most cases the data was cut to avoid such edge effects as discussed in Section 2.2.2. The same is true for

---

<sup>7</sup> A brick is a  $1.5^\circ \times 3^\circ$  region as discussed in Shectman et al. 1996

plates 300, 301 & 344 (regardless of LCRS declination slice) since these three plates are at the corners of the EDSGC where the number of plate overlaps is significantly smaller than for other plates; plate 300 only overlaps with plate 301 which in turn only overlaps with plates 357 & 299. For plate 301, the measured magnitude offset with these overlapping plates is  $\Delta m_{301-357} = 0.35$  and  $\Delta m_{301-299} = 0.11$  *i.e.* the average magnitude difference for galaxies in common between two plates. This may explain the larger scatter seen for plates 300 & 301 since they are somewhat isolated from the rest of the EDSGC (they are on the southeast corner of the EDSGC). Similarly, Plate 344 is on the southwestern corner of the EDSGC and also suffers from a smaller number of plate overlaps with other plates; it only overlaps with plate 405 ( $\Delta m_{344-405} = 0.028$ ) and plate 345 ( $\Delta m_{344-345} = -0.05$ ).

We note that the feature in Figures 1 & 2 near Plate 293 could be due to real large-scale structure. As shown in Guzzo et al. (1992), this area of the EDSGC coincides with both the Sculphor and BS1 superclusters; two of the largest superclusters presently known.

Finally, we have also carried out a similar analysis using the 907 galaxies in common between the ESO Nearby Abell Cluster Survey (ENACS; Katgert et al. 1996) and the EDSGC (ENACS provides a R-band magnitude for all their galaxies). The results are the same as above with the LCRS in that the mean  $b_j - R$  color for EDSGC-ENACS galaxies is a near constant as a function of right ascension.

## 5.2. Star–Galaxy Separation

As discussed in Section 4, the EDSGC has been used for several large galaxy redshift surveys. A by-product of this work is an external check on the star–galaxy separation techniques of the EDSGC since stars are easy to spectroscopically differentiate from galaxies. The best test of this comes from the ESO Slice Project (Vettolani et al. 1997)

since they targeted for spectroscopic observations all  $b_j \leq 19.4$  EDSGC galaxies between a right ascension of  $22.5^h$  and  $1^h 20^m$  at a mean declination of  $-40.25^\circ$ . From this sample, which is 90% complete in observations, only 12% of EDSGC galaxies were stars. This is slightly higher than we observed from our visual checks (Heydon-Dumbleton et al. 1989 quotes  $< 10\%$ ) of the star–galaxy separations discussed above in Section 2.1.1.

## 6. Discussion

In this section we give a brief review of the science to originate from the EDSGC:

### 6.1. Galaxies

The angular correlation function ( $w(\theta)$ ) of the EDSGC and its stability to Galactic extinction and photometric calibration errors are given in CNL92 and Nichol & Collins (1993) respectively. These results confirm the high amplitude of the angular correlation function found by the APM survey (Maddox *et al.* 1990b) and help demonstrate that the previous results pertaining to the Lick galaxy catalogue (Groth & Peebles 1977) were in error. Higher order correlations have been analysed by Szapudi, Meiksin & Nichol (1996) which are in good agreement with predictions from N-body simulations and suggest that the galaxies are reliable tracers of the underlying mass distribution. A comparison of the large-scale clustering in the APM and EDSGC galaxy surveys was performed by Szapudi & Gaztanaga (1998). On large angular scales the main difference between counts in cells is attributable to the smaller area, and therefore greater edge effects, of the EDSGC compared to the APM. On small scales there is evidence that the EDSGC follow N-body simulations more closely than APM which could be a result of the EDSGC de-blending algorithm. However, none of the differences detected effect the results on large-scale structure or their

interpretations as published by the two groups.

The EDSGC has been the parent galaxy catalogue for two extensive redshift surveys: the ESO Slice Project (ESP) and the Durham/UKST Galaxy Redshift Survey. The ESP is an 85% complete galaxy redshift survey consisting of  $\sim 3300$  galaxies brighter than  $b_j = 19.4$  in a 23.3 square degree region close to the South Galactic Pole (Vettolani *et al.* 1997). Most notable are the results on the luminosity function and mean galaxy density (Zucca *et al.* 1997) which provide clear evidence for a “local” underdensity in the galaxy distribution out to  $\sim 140 \text{ h}^{-1} \text{ Mpc}$ . Along with the Las Campanas (Shectman *et al.* 1996) and Stromlo-APM (Loveday *et al.* 1996) redshift surveys, the ESP project provides one of the most accurate estimates of the faint end of the galaxy luminosity function. The Durham/UKST Galaxy Redshift Survey consists of a one-in-three sampled survey of  $\sim 2500$  galaxies to  $b \leq 17$  covering the EDSGC area (Ratcliffe *et al.* 1998). The results of this survey suggest that both the structures on scales  $50\text{-}100 \text{ h}^{-1}\text{Mpc}$  and the smaller scale pairwise galaxy velocity dispersion show significant power in excess of the predictions of the standard cold dark matter model. Finally, Knox, Huterer & Nichol (2000) have used this extensive redshift data to compute an angular power spectrum, and its covariance matrix, for the whole EDSGC data and compare these results to cosmological predictions.

## 6.2. Clusters

The work on galaxy clusters from the EDSGC has been particularly productive and includes: publication of the first machine-based cluster catalogue – the EDCC (Lumsden *et al.* 1992); results on the spatial distribution and correlation function of clusters (Guzzo *et al.* 1992, Nichol *et al.* 1992); an analysis of the alignments of galaxy clusters (Martin *et al.* 1995); a study of the cluster galaxy luminosity function from the largest single database ever used to study this problem (Lumsden *et al.* 1997); a comprehensive redshift survey of

rich clusters (Collins *et al.* 1995). In addition, the EDSGC has been used recently to study the local space density of optical clusters (Bramel, Nichol & Pope 2000) and the relationship between optical and X-ray luminosities of clusters (Miller, Melott & Nichol 2000).

## 7. Acknowledgments

We are grateful to the COSMOS and UK Schmidt units at the Royal Observatory Edinburgh and Anglo–Australian Observatory for their continued support of the EDSGC. We would also like to thank PPARC for their financial support of the EDSGC. We are indebted to Neil Heydon-Dumbleton and Luigi Guzzo for their help and advice over the lifetime of this project and we thank Matthew Colless for making his CCD calibration data available to us. Finally, we thank Marion Schmidt of the NASA/IPAC Extragalactic Database (NED) for his continuing checks of the EDSGC. This work was sponsored in part by NASA grant NAG5-3202 (RCN).

## REFERENCES

- Abell, G. O., 1958, *ApJS*, 3, 211
- Abell, G. O., Corwin, H. G. Jr., Olowin, R. P., 1989, *ApJS*, 70, 1
- Beard, S. M., MacGillivray, H. T., Thanisch, P. F., 1990, *MNRAS*, 247, 311
- Bramel, D. G., Nichol, R. C., Pope, A. C., 2000, *ApJ*, accepted (astro-ph/9912275)
- Bruck, M. T., Waldron, J. D., 1984, *Astronomical Photography*
- Cannon, R. D., Hawarden, T. G., Sim, E., Tritton, S. B., 1978, Royal Observatory, Edinburgh (Scotland).
- Collins, C. A., Heydon-Dumbleton, N. H., Macgillivray, H. T., 1989, *MNRAS*, 237, 7
- Collins, C. A., Nichol, R. C., Lumsden, S. L., 1992, *MNRAS*, 254, 295 (CNL92)
- Collins, C. A., Guzzo, L., Nichol, R. C., Lumsden, S. L., 1995, *MNRAS*, 274, 1071
- Djorgovski, S. G., Gal, R. R., Odewahn, S. C., de Carvalho, R. R., Brunner, R., Longo, G., Scaramella, R., 1998, in *Wide Field Surveys in Cosmology*, eds. S. Colombi and Y. Mellier
- Geller, M. J., Kurtz, M. J., de Lapparent, V., 1984, *ApJ*, 287, L55
- Guzzo, L., Collins, C. A., Nichol, R. C., Lumsden, S. L., 1992, *ApJ*, 393L, 5
- Heydon-Dumbleton, N. H., Collins, C. A., Macgillivray, H. T., 1989, *MNRAS*, 238, 379
- Heydon-Dumbleton, N. H., 1989, PhD. Thesis, Univ. of Edinburgh
- Katgert, P., Mazure, A., Perea, J., den Hartog, R., Moles, M., Le Fevre, O., Dubath, P., Focardi, P., Rhee, G., Jones, B., Escalera, E., Biviano, A., Gerbal, D., Giuricin, G., 1996, *A&A*, 310, 8

- Knox, L., Huterer, D., Nichol, R.C., 2000, ApJ, in preparation
- Loveday, J., Peterson, B. A., Maddox, S. J., Efstathiou, G., 1996, ApJS, 107, 201
- Lumsden, S. L., Nichol, R. C., Collins, C. A., Guzzo, L., 1992, MNRAS, 258, 1
- Lumsden, S. L., Collins, C. A., Nichol, R. C., Eke, V. R., Guzzo, L., 1997, MNRAS, 290, 119
- MacGillivray, H. T., Stobie, R. S., 1984, Vistas in Astronomy, 27, 433
- MacGillivray, H. T., Dodd, R. J., 1982, Astrophysics and Space Science, 83, 127
- Maddox, S. J., Efstathiou, G., Sutherland, W. J., Loveday, J., 1990b, MNRAS, 242, 43
- Maddox, S. J.; Efstathiou, G.; Sutherland, W. J., 1990a, MNRAS, 246, 433
- Martin, D. R., Nichol, R. C., Collins, C. A., Lumsden, S. A., Guzzo, L., 1995, MNRAS, 274, 623
- Miller, C. J., Melott, A. L., Nichol, R. C., 2000, ApJ, submitted (astro-ph/9912362)
- Nichol, R. C., Collins, C. A., Guzzo, L., Lumsden, S. L., 1992, MNRAS, 255, 21P
- Nichol, R. C., 1993, PhD. Thesis, Univ. of Edinburgh
- Nichol, R. C., Collins, C. A., 1993, MNRAS, 265, 867
- Miller, L., Cormack, W., Paterson, M., Beard, S., Lawrence, L., 1991. "Digitised Optical Sky Surveys", eds. H.T. MacGillivray and E.B. Thomson, Kluwer Academic Publishers
- Phillipps, S., Parker, Q.A., Schwartzberg, J.M., Jones, J. B., 1998, ApJ, accepted.
- Ratcliffe, A., Shanks, T., Parker, Q. A., Broadbent, A., Watson, F. G., Oates, A. P., Collins, C. A., Fong, R., 1998, MNRAS, 300, 417



- Shectman, S. A., Landy, S. D., Oemler, A., Tucker, D. L., Lin, H., Kirshner, R. P., Schechter, P. L. 1996, ApJ, 470, 172
- Stobie, R. S., 1980, British Interplanetary Society, Journal (Image Processing), 33, 323
- Szapudi, I., Meiksin, A., Nichol, R.C., 1996, ApJ, 473, 15
- Szapudi, I, Gaztanaga, E., 1998, MNRAS, 300, 493
- Vettolani, G., Zucca, E., Zamorani, G., Cappi, A., Merighi, R., Mignoli, M., Stirpe, G. M., MacGillivray, H., Collins, C., Balkowski, C., Cayatte, V., Maurogordato, S., Proust, D., Chincarini, G., Guzzo, L., Maccagni, D., Scaramella, R., Blanchard, A., Ramella, M., 1997, A&A, 325, 954
- York, D. G., *et al.* (SDSS Collaboration), AJ, submitted (technical description of the SDSS)

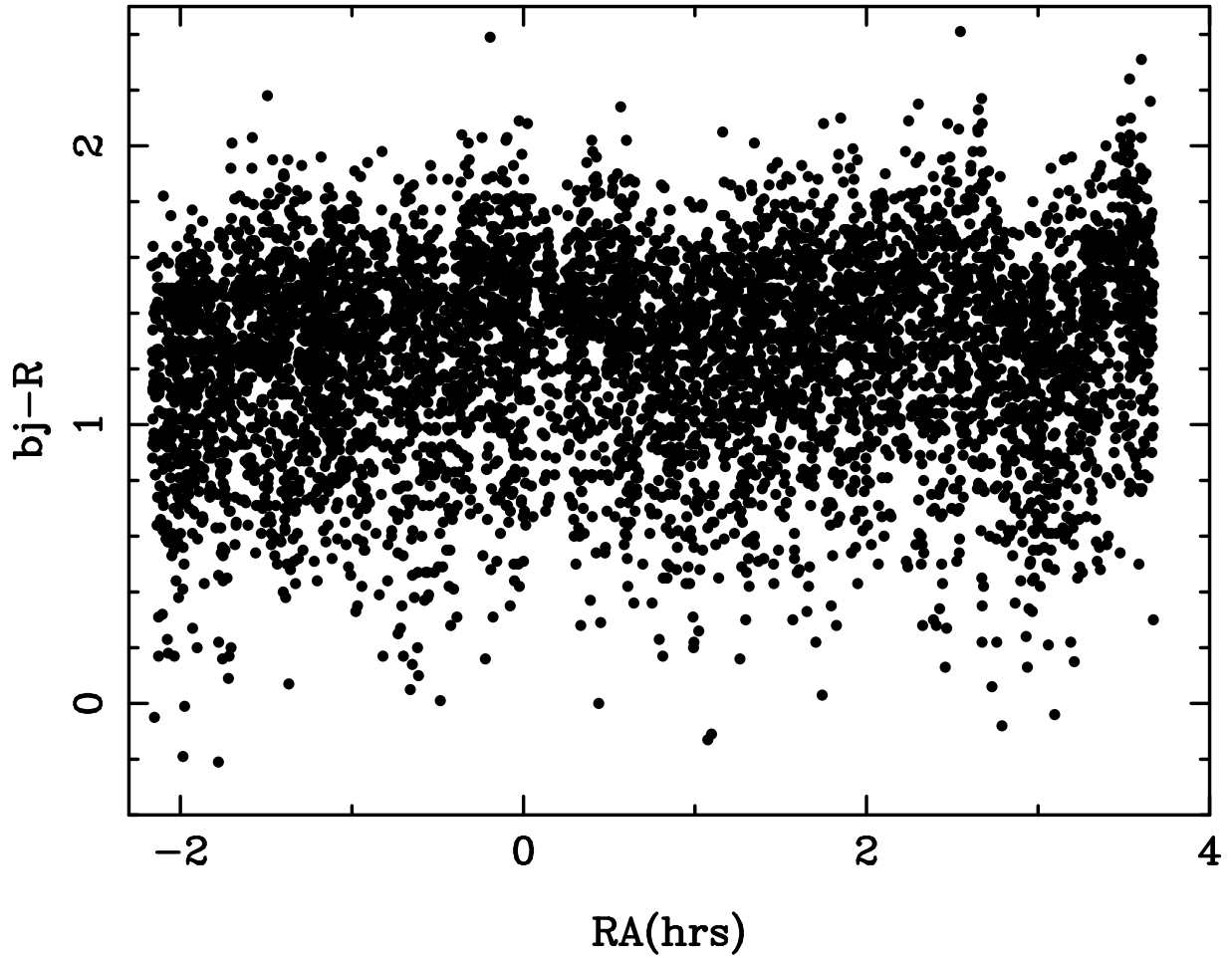


Fig. 1.— We present here the  $b_j - r$  color for all 5996 galaxies in common between the EDSGC and LCRS as a function of the EDSGC right ascension of the galaxy. We have made no cuts on the data.

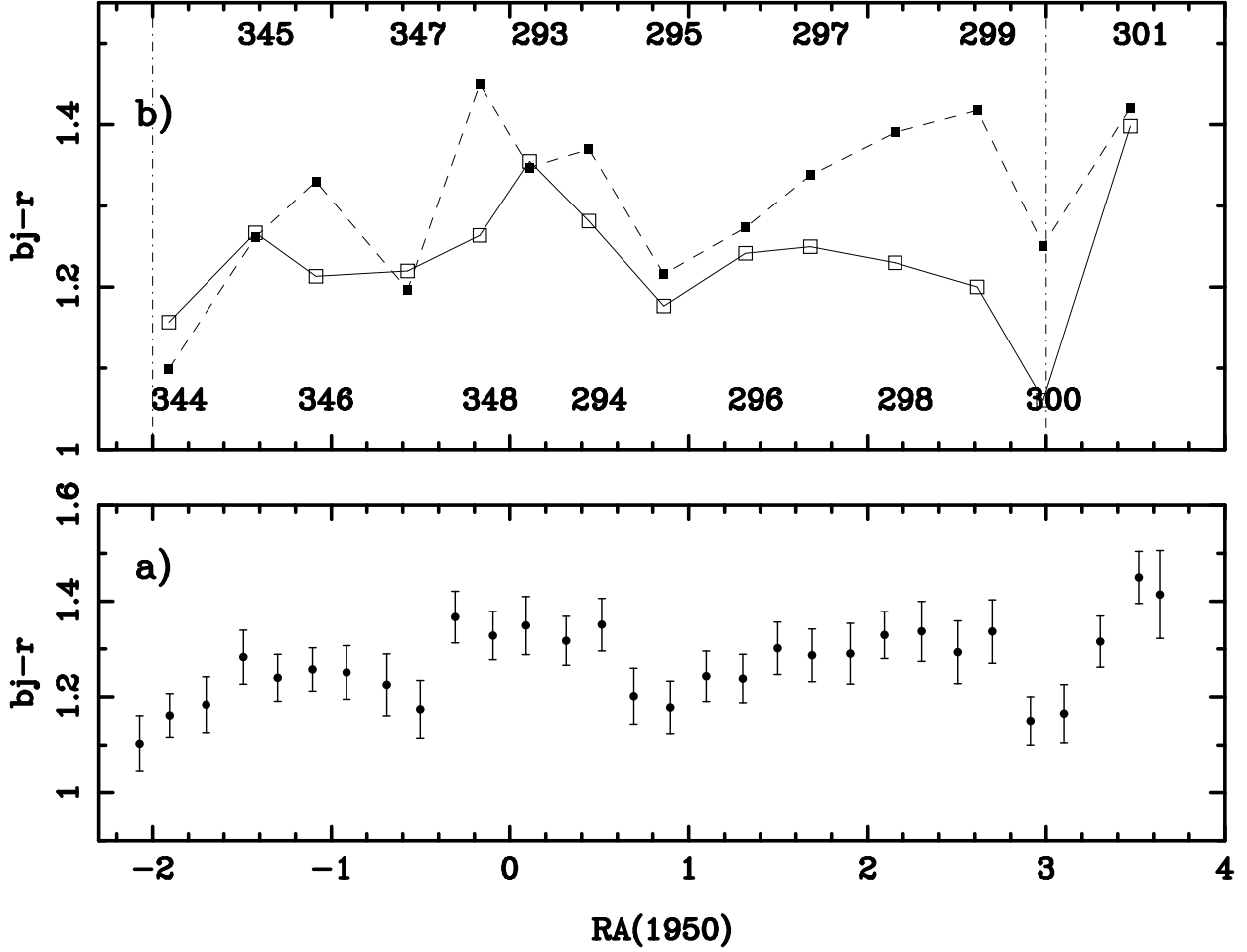


Fig. 2.— In panel a), we present the mean, and standard error on the mean, of the  $b_j - r$  color for all EDSGC-LCRS galaxies in the EDSGC magnitude range  $17 < b_j < 20$  as a function of the EDSGC right ascension of the galaxy. In this magnitude range, the EDSGC is considered to be free of systematic problems like saturation of galaxy cores (see Lumsden et al. 1997) as well as being well above the flux limit of the photographic plates. In panel b), we plot the same data as shown in panel a) but now as a function of plate identification number *i.e.* we present the mean  $b_j - r$  color for all EDSGC-LCRS galaxies on a given plate. We plot the color data versus the mean right ascension of the plate. The solid square symbols are for galaxies in the  $-42^\circ$  LCRS declination slice while the open square symbols are for the  $-39^\circ$  LCRS declination slice. The plate identification number for each pair of points is given either above or below the data (to avoid overcrowding on the plot). The lines are presented to aid the reader and have no scientific rationale. The dot-dashed vertical lines are the limits of the EDSGC as discussed in Section 3.

Table 1: The EDSGC plates with CCD Sequences

Plate No.	$m_{sky}$	Plate No.	$m_{sky}$	Plate No.	$m_{sky}$
293	$22.14 \pm 0.04$	294	$22.31 \pm 0.04$	296	$22.20 \pm 0.04$
298	$22.41 \pm 0.05$	300	$22.34 \pm 0.05$	342	$22.35 \pm 0.03$
344	$21.77 \pm 0.06$	346	$22.17 \pm 0.03$	347	$22.24 \pm 0.05$
348	$22.25 \pm 0.06$	349	$21.77 \pm 0.02$	351	$22.48 \pm 0.06$
353	$22.39 \pm 0.04$	355	$22.00 \pm 0.07$	405	$22.22 \pm 0.04$
407	$22.14 \pm 0.04$	410	$22.58 \pm 0.03$	411	$21.61 \pm 0.04$
412*	$22.40 \pm 0.07$	414	$22.27 \pm 0.05$	416*	$22.03 \pm 0.03$
466	$22.10 \pm 0.05$	468	$22.43 \pm 0.06$	469	$22.00 \pm 0.05$
470	$22.13 \pm 0.05$	471*	$22.42 \pm 0.05$	472	$22.40 \pm 0.04$
474	$21.97 \pm 0.04$	477	$22.11 \pm 0.04$	531	$21.93 \pm 0.04$
533	$21.95 \pm 0.04$				

Table 2: Ten Interactive Drill Holes within the Boundaries of the EDSGC

RA (hrs)	DEC(Degrees)	Drill Diameter (arc mins)	Comments
22.9142	-29.89392	40.90	HD 216956, a bright star
23.0850	-30.04382	40.90	large plate error
23.5302	-36.37440	5.6	IC5332
23.9943	-30.00320	8.61	HD 224990, a bright star
0.08746	-37.92240	18.00	NGC 0300, a bright galaxy
0.09624	-34.00000	25.00	the Sculpter Dwarf Elliptical
0.8373	-31.46767	6.48	NGC289/ARP 81
0.8390	-26.85695	12.90	Near NGC 288/Globular cluster
0.8824	-37.82746	9.75	Near NGC 0300
2.6292	-34.71350	40.00	the Fornax Dwarf Spheroidal

Table 3: The Seven Attributes in the Small Version of the EDSGC

Name	Units	Description
RA	Hours	Right Ascension (B1950)
DEC	Degrees	Declination (B1950)
MAGNITUDE	Magnitudes	Calibrated $b_j$ magnitude
PLATE ID	No units	The UK Schmidt Field ID number
IMAJAX	Arcseconds	Intensity weighted semi-major axis
IMINAX	Arcseconds	Intensity weighted semi-minor axis
POSANGLE	Degrees	Position angle on the sky

Table 4: The Twenty Seven Attributes in the Full EDSGC

Name	Units	Description
RA	Hours	Right Ascension (B1950)
DEC	Degrees	Declination (B1950)
XMIN	0.1 microns	x–coordinate minimum of source
XMAX	0.1 microns	x–coordinate maximum of source
YMIN	0.1 microns	y–coordinate minimum of source
YMAX	0.1 microns	y–coordinate maximum of source
AREA	pixels	Measured area of the source
IMAX	intensity	Maximum intensity above sky value
COSMAGCAL	magnitudes	COSMOS or instrumental magnitude
ISKY	intensity	Sky intensity at centroid
IXCEN	0.1 microns	Intensity weighted x–centroid
IYCEN	0.1 microns	Intensity weighted y–centroid
UMAJAX	0.1 microns	Unweighted semi–major axis
UMINAX	0.1 microns	Unweighted semi–minor axis
UTHETA	Degrees	Unweighted orientation
IMAJAX	0.1 microns	Intensity weighted semi–major axis
IMINAX	0.1 microns	Intensity weighted semi–minor axis
POSANGLE	Degrees	Position angle on the sky
CORMAGCAL	Magnitudes	COSMOS classification flag (internal use only)
SIGMA	$\sqrt{\text{pixels}}$	Gaussian fit parameter (see Section 2)
IDSEQ	No units	Sequential ID number
LOGAREA	Log(pixels)	Logarithm of Area (see Section 2)
GEOM	No units	Geometric parameter (see Section 2)
GEOMLOG	No units	GEOM*LOGAREA
PLATE ID	No units	The UK Schmidt Field ID number
MAGNITUDE	magnitudes	Calibrated $b_j$ magnitude
SPARE	No units	Spare Attribute